ORIGINAL PAPER

Production and Characterization of Gelatin Spherical Particles Formed via Electrospraying and Encapsulated with Polyphenolic Antioxidants from *Momordica charantia*

Amir Ehsan Torkamani[1] · Zainul Abidin Syahariza[1] · Mohd Hani Norziah[1] · Wan Ahmad Kamil Mahmood[2] · Pablo Juliano[3]

Abstract

This study dealt with the production and characterization of gelatin nanospheres and encapsulation with *Momordica charantia*, commonly known as bitter gourd fruit vegetable extract (BGE). The impact of encapsulation and increasing the encapsulate loading on various physiochemical characteristics of gelatin polymeric entities as well as antioxidative attributes of BGE was studied. Nanospheres were formed via an electrospraying process conducted at 20 kV, 0.5 mL/h, and 10 cm of voltage, flow rate, and emitter/collector distance, respectively. The spherical beads were encapsulated with BGE at 5 to 15% ($w/w\%$) loading rate. Morphological analysis through scanning electron microscopy (SEM) and atomic force microscopy (AFM) demonstrated that nanospheres could be successfully produced. Furthermore, nanosphere encapsulation of the extract was demonstrated in transmission electron microscope (TEM) micrographs. Spectroscopic analysis indicated no chemical interactions between core and wall materials. The thermal stability of encapsulated nanoparticles slightly increased and the glass transition temperature (T_g) disappeared due to increased crystallinity. Thermogravimetric graphs of encapsulated spherical beads, at all core loadings, showed an additional phase ranging from 138 to 249 °C, overlapping with the BGE's main TGA degradation phase. The presence of this phase, which was absent from empty bead thermograms, confirmed encapsulation occurrence during electrospraying process. Furthermore, an average of 80% of antioxidative content and potency of the extract was conserved during the encapsulation process. Moreover, phenolic content and antioxidative activity of the encapsulated extract showed higher stability than extracts while stored at refrigerated and ambient conditions.

Keywords Electrospraying · Spherical bead · Nano-encapsulation · Gelatin · Bitter gourd · Non-thermal technology

---

✉ Zainul Abidin Syahariza
   syahariza@usm.my

1   Food Technology Department, School of Industrial Technology, Universiti Sains Malaysia, 11800 Minden, Penang, Malaysia

2   School of Chemical Sciences, Universiti Sains Malaysia, 11800 Minden, Penang, Malaysia

3   CSIRO Agriculture and Food, 671 Sneydes Road, Werribee, VIC 3030, Australia

Introduction

The use of natural biodegradable polymeric encapsulants to increase the storage stability of nutraceutical compounds have gained much attention within the past decade (Xu and Hanna 2006; Pérez-Masiá et al. 2015). Encapsulation can essentially extend the stability of bioactive compounds as well as their beneficial functionalities during storage. A range of different techniques is being used to encapsulate bioactive compounds at micron, sub-micron, and nano-scales. Among these methods, spray drying, emulsification-crosslinking, coacervation, and emulsification-evaporation are more commonly and extensively used (Gharsallaoui et al. 2007; López-Rubio et al.

2012; Gómez-Mascaraque et al. 2015; Ezhilarasi et al. 2013). Despite their benefits, these methods possess various drawbacks making them not entirely suitable and compatible with the bioactive compounds (López-Rubio and Lagaron 2011). In all of the mentioned methods, the bioactive compounds are exposed to high temperatures and organic solvents during the production process (López-Rubio and Lagaron 2011). Extensive heating could adversely affect the chemical integrity of thermolabile compounds and reduce its stability and functional activity (Rocío Pérez-Masiá et al. 2015). The existence of organic solvents in trace quantities within the encapsulated structure could prohibit its application for food/pharmaceutical purposes due to toxicity (Birnbaum et al. 2000; López-Rubio et al. 2012). These issues resulted in a search for more simple, versatile, and accelerated encapsulation methods that eliminate the requirement of heating stage.

Electrospraying (electrohydrodynamic atomization) is considered as a sister technology to electrospinning, following similar principles although with some variations (Anu Bhushani and Anandharamakrishnan 2014). During the electrospraying process, the spinning process is interrupted resulting in atomization of the charged liquid polymer. This issue is mainly due to alteration of the solution properties, mainly solution concentration as well as flow rate and applied voltage (Kriegel et al. 2009). Low polymer concentration results in dominance of surface tension repulsion over viscoelastic forces, leading to bead formation, jet destabilization, viscose instability and formation of fine self-dispersing droplets (Jaworek and Sobczyk 2008). Very few studies have dealt with encapsulation of pure bioactive compounds within biopolymers via electrospraying method. Gómez-Estaca et al. (2015) reported that encapsulated curcumin within gelatin microspheres had better water solubility, antioxidative, color dispersion and bio-accessibility properties in comparison to commercial samples. Pérez-Masiá et al. (2014) studied the electrosprayability of various water-soluble food grade hydrocolloids, to compare and benchmark polymers as potential encapsulating matrices. They showed that addition of gums and surfactants to the biopolymeric solutions improved their sprayability and dispersibility. Bakhshi et al. (2013) optimized electrospraying encapsulation process of folic acid within sodium alginate. Gómez-Mascaraque et al. (2015) encapsulated (−)-epigallocatechin gallate (EGCG) using electrospraying process, demonstrating a near 100% encapsulation efficiency and antioxidant activity retention. López-Rubio and Lagaron (2012) showed that encapsulation of β-carotene within whey protein concentrate (WPC) microcapsules significantly improved its photo-oxidative stability. The possibility of encapsulation of a model crude extract obtained from Moringa leaves within spherical structures using electrospraying has also been investigated by Hani et al. (2016). However, to the best of authors knowledge, no study has systematically dealt with nano or submicron encapsulation of an extract obtained from the edible part of a fruit-like vegetable model via electrospraying method.

Bitter gourd (BG) plant has been chosen as a model fruit vegetable due to its popularity within the tropical region as a herbal medicine and its high antioxidative properties (Kenny et al. 2013; Lin et al. 2011; Dandawate et al. 2016). It has been shown that the antioxidant potent BGE has a therapeutic effect on patients with polydipsia, diarrhea, colic, infections and diabetes (Fang et al. 2012). Furthermore, the extract obtained from the edible part of BG through near critical accelerated extraction illustrated significant antioxidative potency in comparison to other conventional methods (Budrat and Shotipruk 2009; Syahariza et al. 2017).

This study firstly investigated the production of nanosphere gelatin particles sourced from the fish skin which often discarded as industrial waste. Secondly, encapsulation of BGE obtained through pressurized liquid extraction (PLE) and its effect on morphological, spectroscopic and thermal properties of obtained spherical structures. Eventually, the phenolic compound and its antioxidative stability at various environmental conditions namely storage temperature and relative humidity were evaluated over an extended period of time. In other word, the main objectives of the current research were (1) to investigate the possibility and produce gelatin bead films (consisted of nanospheres) and encapsulate them via electrospraying at ambient conditions and (2) to investigate the physiochemical characteristics of gelatin, as encapsulating polymer, following nonthermal encapsulation and increasing the encapsulate loading as well as antioxidative attributes of BGE.

Materials and Methods

Chemicals and Reagents

Ethanol, methanol, Folin-Ciocalteau reagent, gallic acid, quercetin, ferrous sulfate, 2,2-diphenyl-1-picrylhydrazyl (DPPH), 2,4,6-tripyridyl-s-triazine (TPTZ), sodium carbonate, ferric (III) chloride hexahydrate, aluminum trichloride and glacial acetic acid were purchased from Merck Millipore (Billerica, MA, USA). Deionized water (18.2 mΩ cm) was generated in-house using a purifier (ELGA Purelab Option-Q, ELGA LabWater, High Waycomb, BUX, UK). The bitter gourd extract (BGE) was obtained in-house using an accelerated solvent extractor as described previously by Syahariza et al. (2017). The antioxidative properties of BGE was defined by total phenolic content (TPC) of 5.40 ± 0.30 g GAE/100 g, total flavonoid content (TFC) of 1.50 ± 0.10 g QE/100 g, ferric reducing/antioxidant power (FRAP) of 778.55 ± 10 μmol eq Fe (II)/g and radical scavenging activity using half maximal inhibitory concentration (RSA-IC$_{50}$) of 0.06 mg/mL. Fish gelatin was extracted from tilapia fish skins (*Oreochromis*

mossambicus) following methods as described in our previous work by Norziah et al. (2009) and Zhou and Regenstein (2005). In brief, the fish skin was mixed with 0.2 M $Ca(OH)_2$ (fish skin: $Ca(OH)_2$, 1:6) for 1 h followed by 0.1 M citric acid (fish skin: citric acid,1:6) for 3 h. Eventually, extraction with distilled water (fish skin: water, 1:2) at 50 °C for 3 h and washing with water were carried out after each treatment. Eventually, the extract was filtered using a cheese cloth and drying was performed at 70 °C using an oven dryer. The bloom strength of the extracted fish gelatin was determined following the standard test method described by Gelatin Manufacturers Institute of America (GMIA 1986) in triplicates, which was 284 g. The obtained gelatin powder was then used as the wall material for the encapsulation process.

Electrospraying System Setup

The electrospraying system setup was assembled in-house and comprised of 3 main components: a high voltage power supply (Spellman CZE1000r, New York, NY, USA); a syringe pump (New Era NE-1000, New York, NY, USA) and a grounded static plate collector. A 5-mL hypodermic syringe equipped with a blunt tip needle (1.00 mm internal diameter) was used as the emitter. As illustrated in Fig. 1, the emitter system was aligned horizontally against the collector compartment covered with a sheet of aluminum foil with 10 cm of clearance.

Production of Nanoparticles via Electrospraying Technique

Feed Solution Preparation

Required masses of gelatin powder to prepare designated concentrations of the polymer solution was transferred to glass vials containing 2 mL of 30% aqueous acetic acid. The screwcaps were sealed with parafilm and the solutions were stirred for exactly 12 h at ambient conditions till total dissolution was reached.

Electrospraying Process

Preliminary Tests

Electrical potential difference (15 kV, 20 kV and 25 kV) and flow rate (0.25 mL/h, 0.5 mL/h and 0.75 mL/h) values were varied while polymer concentration was maintained at minimum required concentration of 5% for electrospraying. After selecting the most suitable voltage and flow rate, the concentration of the feed polymer was varied to higher concentrations until the morphological and structural consistency of the spherical beads was compromised. The main aim of variable modulation was to obtain uniform spherical particles using least electrical energy and polymer material at shortest processing time possible.

Hollow and Encapsulated Particle Production

After suitable electrospraying condition was selected, encapsulated gelatin nanoparticles were then prepared by incorporating different concentrations of BGE (5 to 30% *w/w* of gelatin with 5% intervals) as the core material. The electrospraying process was performed in triplicates for each set of concentration.

Scanning Electron Microscopic Analysis

Exterior morphology of nanostructures was observed by a field emission scanning electron microscopy (FE-SEM) at high vacuum with an Everhart-Thornley detector (ETD, QUANTA FEG 650 2012, Baverton, OR, USA). The beam voltage, working distance and coating material were 10 kV, 7.4 mm and chromium, respectively. The particle size and its distribution for each specimen were statistically analyzed using Minitab 17.2.0 (Minitab Ltd., Coventry, WMD, UK) to obtain mean diameter and their respective histograms.

Transmission Electron Microscopic Analysis

Nanoparticles were directly electrosprayed and coated on the copper grid; Transmission electron microscopy was conducted using a Zeiss Libra120 (Carl Zeiss AG, Oberkochen, BW,
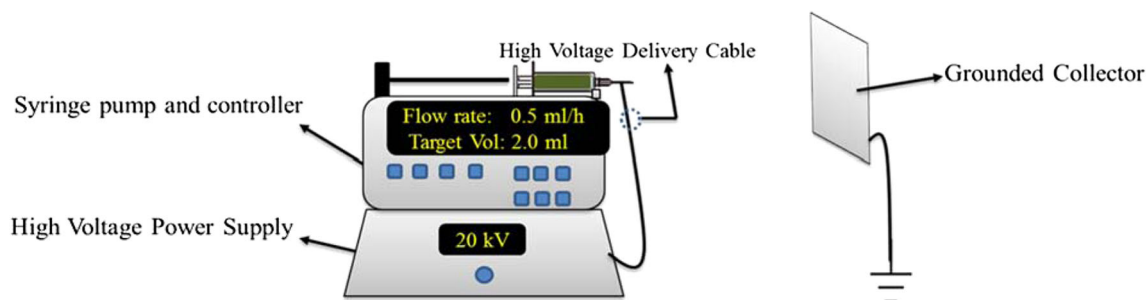
Fig. 1 Schematic view of the electrospinning system setup

Germany) with an Olympus image analysis software to observe the interior morphology.

Atomic Force Microscopic Analysis

Atomic force microscopy images of the nanoparticles were obtained using AFM system (Dimension Edge, Bruker, Billerica, MA, USA) to capture three-dimensional topographical images of the surface of the nanoparticles. Surface topographical analysis of nanoparticles was obtained through tapping mode and the surface roughness was calculated with a NanoScope analysis software version 1.40. The surface roughness was reported as the root-mean square average of height deviations taken from the mean data plane (Rq) and average of the absolute value of the height deviations from a mean surface (Ra).

Encapsulation Efficiency Determination

Encapsulation efficiency (EEF) of BGE loaded nanoparticles were determined using TPC, TFC, FRAP and RSA-IC$_{50}$ values as the indicative measurement. The encapsulated nanoparticle films were initially dissolved in 5 mL of 40% methanol solution followed by centrifugation at 3500 rpm for 3 min. After precipitation of gelatin, the supernatant was collected and analyzed for phenolic/flavonoid content as well as antioxidant potency as described by Syahariza et al. (2017). The percentage EEF of encapsulated BGE in the nanoparticle was determined as a ratio of TPC, TFC, FRAP and RSA-IC$_{50}$ of encapsulated BGE to their non-encapsulated counterparts multiplied by hundred.

Attenuated Total Reflectance Fourier Transform Infrared Spectroscopic (ATR-FTIR) Analysis

Functional groups and probable chemical interactions in nanoparticles were determined using ATR-FTIR spectrometer (Perkin Elmer, Waltham, MA, USA). A scanning range of 4000 to 400 cm^{-1} with a resolution of 0.4 cm^{-1} was applied. The spectrum for each sample was obtained after a total of 16 scans.

Thermogravimetric Analysis

Thermogravimetric analysis (TGA) was carried out using a TGA/SDTA851 thermogravimetric analyzer (Mettler Toledo, Columbus, Ohio, USA) where samples (5 mg) were heated from 25 to 900 °C at a heating rate of 20 °C/min under an atmosphere of nitrogen gas. The weight loss of the sample against temperature change was recorded and plotted.

Differential Scanning Calorimetry (DSC)

Thermal properties of nanoparticles were obtained using DSC (Perkin Elmer Pyris 1 2000, Waltham, MA, USA) under nitrogen gas flow. The test samples (6–9 mg) were weighed into aluminum pans and were hermetically sealed. Heating, cooling and reheating scans were performed from 30 °C to 250 °C and 300 °C to − 50 °C. A secondary heating cycle up to 300 °C after the cooling cycle was undertaken. Heating and cooling cycles both were performed at 20 °C /min of temperature change rate and were followed by a 1-min holding stage at their endpoint temperatures. An empty aluminum pan was used as a reference.

The degree of crystallinity was calculated by the equation below:

$$X_C = \frac{\Delta H - \Delta H_a}{\Delta H_m^\circ} = \frac{\Delta H_m}{\Delta H_m^\circ} \tag{1}$$

where ΔH_m ($\Delta H - \Delta H_a$) is the enthalpy of melting for gelatin polymer, ΔH_m° is the enthalpy of fusion for 100% crystalline gelatin polymer (62.05 J/g) (Hani et al. 2016).

Functional/Shelf Stability of Encapsulated Shell-Core Structure

Antioxidative shelf stability of encapsulated BGE was observed against their non-encapsulated counterparts at refrigerated (4 °C, 15% RH) and ambient (22 °C, 40% RH) conditions. For this purpose, TPC, TFC, FRAP and RSA value of all sample were determined in a 15-day interval for a total of 180 days. These analyses were performed using the same methods as described earlier in the encapsulation efficiency analysis section.

Statistical Design

A two-way analysis of variance (ANOVA) using general linear model with a 95% level of significance (Minitab 16, Minitab Ltd., Coventry, WMD, UK) was performed to specify significance of difference for obtained average bead diameter and homogeneity, encapsulation efficiency and functional/shelf stability due to encapsulation. The post hoc test utilized to separate means was Tukey's honestly significant difference (HSD) test.

Results and Discussion

Surface Morphology and Particle Size Analysis of Beads

Preliminary tests showed that spherical defect free gelatin beads were formed at all conditions except for 15 kV/0.5–

0.75 mL/h and 25 kV/0.75 mL/h (Online Resources 1–3). The most suitable condition was achieved at 20 kV, 0.5 mL/h and 5% of voltage, flow rate and feed concentration, respectively. As illustrated in the table (Online Resource 4), the particles attained at the mentioned condition had the lowest diameter mean and standard deviation value comparatively. The relatively smaller mean and standard deviation indicated the obtained beads had a higher level of the surface to volume ratio and homogeneity, respectively. Furthermore, increasing gelatin concentration to 8% resulted in formation of more uniform spherical beads with better morphological characteristics (Fig. 2b). The subsequent increase in polymer feed concentration to 10 and 15% (Fig. 2c, d) resulted in aggregation and formation of the bead on string structures, respectively. The formation of pure beads or beaded fibers during electrospraying process is governed by surface tension repulsion and viscoelastic forces balance (Fong et al. 1999; Anu Bhushani and Anandharamakrishnan 2014). At relatively lower concentrations, surface tension forces overcome viscoelastic forces resulting in bead formation. However, increasing infeed polymer concentration changes the balance of power in favor to viscoelastic forces; resulting in bead on string formation.
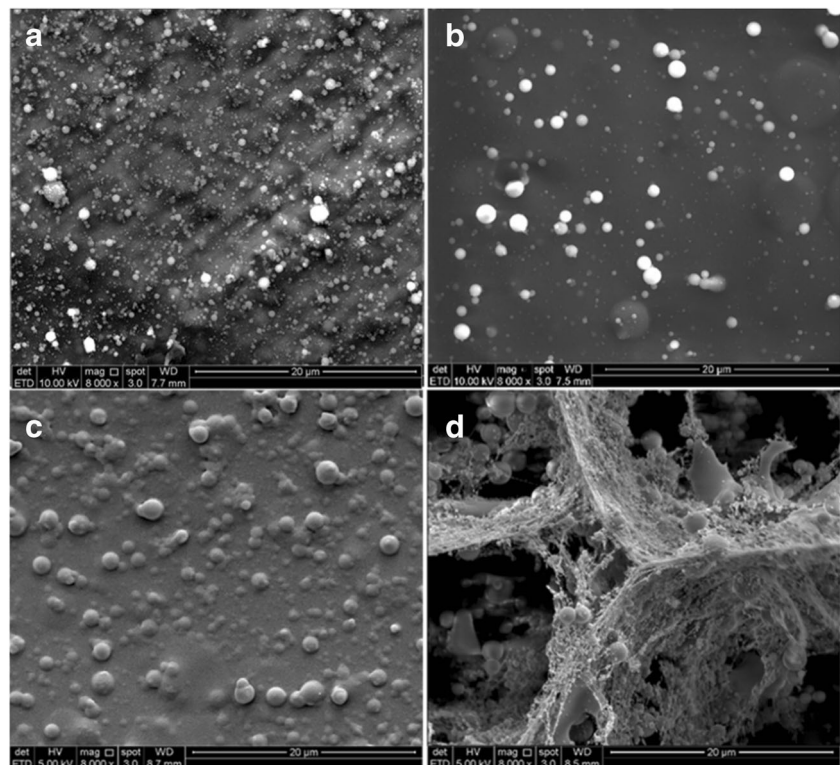
Furthermore, encapsulation of gelatin beads with BGE at 5%, 10 and 15% of wall material content resulted in spherical and fiber-free beads (Fig. 3) whereas at higher concentrations the process was interrupted. As illustrated in Fig. 4, encapsulation process increased the average diameter of particles (ADP) from 269 ± 80 nm in empty gelatin bead (EGB) to 297 ± 70 nm, 1218 ± 250 nm and 1481 ± 320 nm in beads encapsulated at 5% (GBG5%), 10% (GBG10%) and 15% of gelatin wall mass (GBG15%), respectively. The significant ($P < 0.05$) change in ADP occurred during transition from GBG5% to GBG10% while ADP transition from EGB to GBG5% or GBG10% to GBG15% was considered small and insignificant ($P > 0.05$) (Fig. 4a–c). The observed increase in particle diameter especially from 5 to 10% core loading could be due to an increase in the viscosity of in feed solution (Mit-uppatham et al. 2004; Deitzel et al. 2001). Furthermore, distribution of bead diameter as a quantitative indicator of size homogeneity followed the normal distribution trend where 68% of bead diameter value was within $\mu \pm 1\sigma$ range. The broadness of histograms curve fitting significantly ($P < 0.05$) increased, resulting in reduced homogeneity as the core loading increased from 5 to 10%.

Transmission Electron Microscopy

As illustrated in Fig. 5, gelatin beads maintained a uniform spherical shape. The internal diameter of EGB, GBG5%, GBG10% and GBG15% were 270 ± 65 nm, 283 ± 74 nm, 965 ± 130 nm and 1005 ± 150 nm respectively; which is in good agreement with FE-SEM results. The deposition of BGE within the wall material is clearly observed in Fig. 5b–d.

Fig. 2 SEM micrographs of empty gelatin beads at concentrations (*w/v%*) of 5% (**a**), 8% (**b**), 10% (**c**), and 15% (**d**)

Fig. 3 SEM micrographs of gelatin beads without encapsulation (EGB) (**a**), 5% encapsulation (GBG5%) (**b**), 10% encapsulation (GBG10%) (**c**), and 15% encapsulation (GBG15%) (**d**)
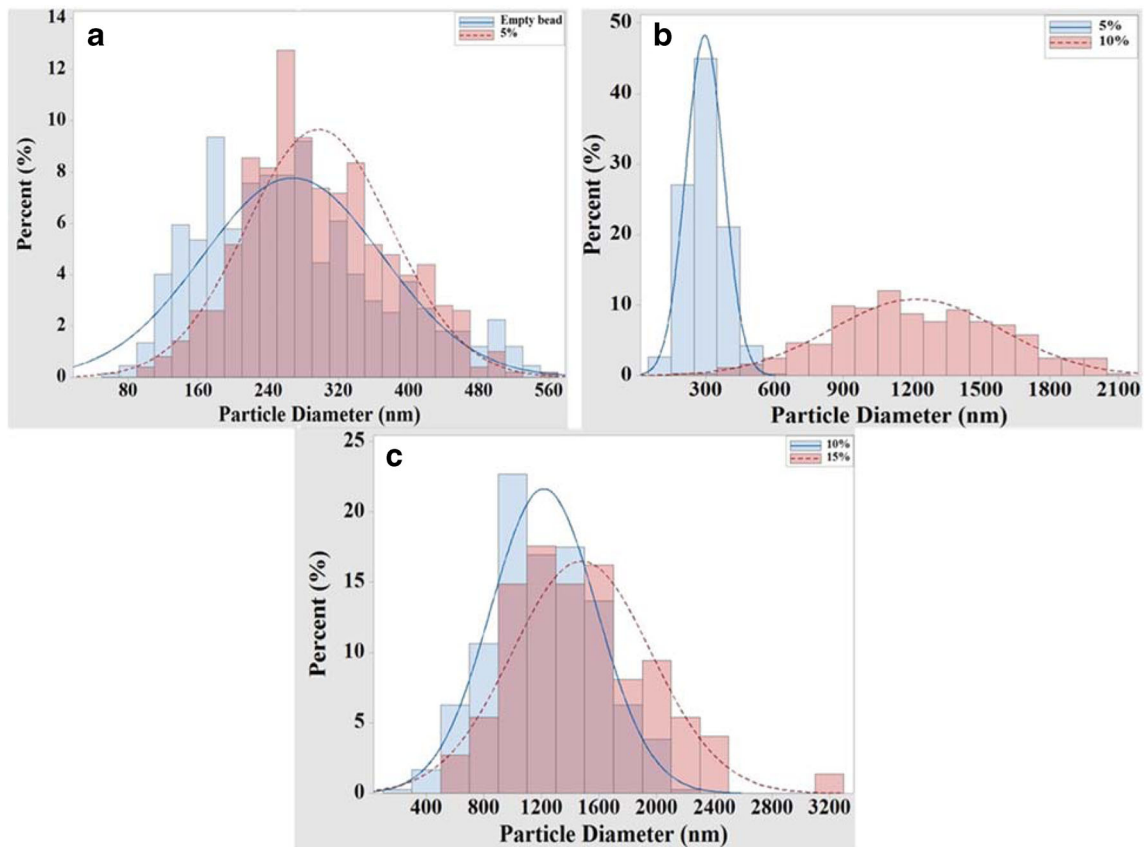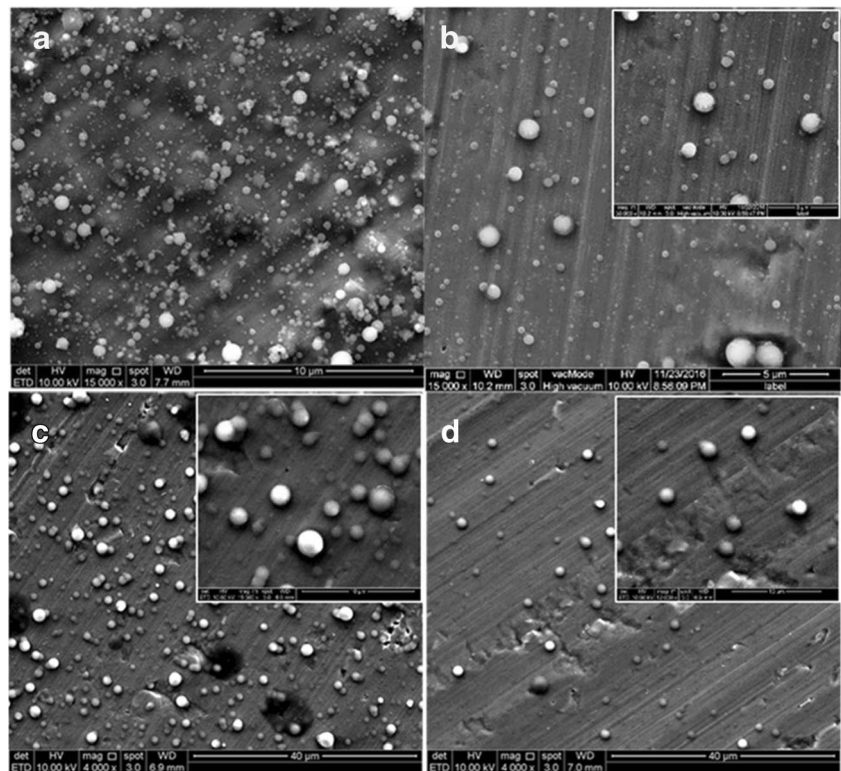
Fig. 4 Particle size distribution of pure gelatin bead (EGB) vs encapsulated beads with 5% extract core loading (GBG5%) (**a**), encapsulated beads with 5% extract core loading (GBG5%) vs encapsulated beads with 10% extract core loading (GBG10%) (**b**), and encapsulated beads with 15% extract core loading (GBG15%) (**c**)

Fig. 5 TEM micrographs of gelatin beads without encapsulation (EGB) (**a**), with 5% core loading (GBG5%) (**b**), with 10% core loading (GBG10%) (**c**), and with 15% core loading (GBG15%) (**d**)
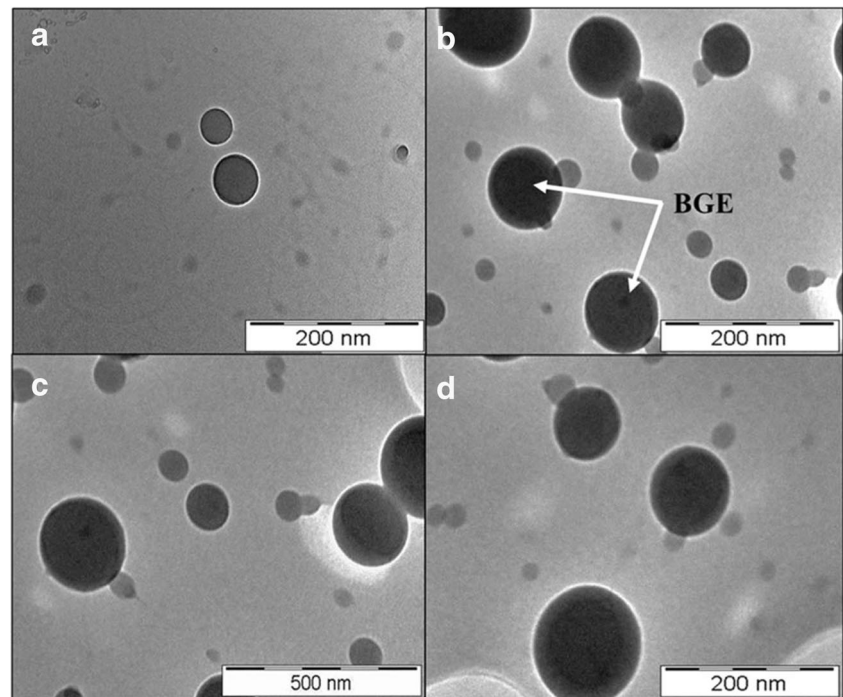
Atomic Force Microscopy

As illustrated in Fig. 6a, pure gelatin beads had a spherical shape which was maintained after encapsulation with BGE (Fig. 6b–d). The morphology of beads obtained from AFM coincided with FE-SEM and TEM micrographs. The surface roughness of EGB, GBG5%, GBG10% and GBG15% were 46 nm, 48 nm, 45 nm and 41 nm respectively, indicating encapsulation process did not alter gelatin films potential coating and adhesion properties.

Encapsulation Efficiency

The EEF of the beads was decided based on total phenolic and flavonoid content of the extract as well as their primary antioxidant properties of FRAP and RSA% (Table 1). The EEF based on TPC, TFC and FRAP ranged from 81 to 84%, 73 to 80% and 85 to 89%, respectively. The RSA-IC$_{50}$ value of encapsulates did not significantly change ($P > 0.05$) and coincided with ranges of the extract. The relatively high EEF of BGE within the gelatin beads could be due to accelerated solidification of the polymer during electrohydrodynamic process.

ATR-FTIR Spectra

The transmittance spectrum of BGE consisted of 11 peaks which ranged from 3284 cm^{-1} to 671 cm^{-1} of frequency (Fig. 7a and Online Resource 5). The spectrum consisted of bands at 3284 cm^{-1} (stretching vibration of phenolic OH group), 2929 cm^{-1} (stretching vibration of aliphatic C-H groups), 1776 cm^{-1} (stretching vibration of C=O group designation to vinyl acetate), 1726 cm^{-1} (stretching vibration of C=O), 1591 cm^{-1} (stretching vibration of aromatic C=C group), 1400 cm^{-1} (bending vibration of aliphatic C-H group), 1040 cm^{-1} (symmetric stretching vibration of C=O group) and 878–671 cm^{-1} (bending vibration of aromatic ring C-H group).

Furthermore, FTIR spectrum of EGB and GBG5 to15% consisted of 9 peaks ranging from 3285 cm^{-1} to 1090 cm^{-1} (Fig. 7b–e and Online Resource 6). A total of 5 characteristic peaks associated with amide vibrations at 3285 cm^{-1} (Amide A), 3047 cm^{-1} (Amide B), 1630 cm^{-1} (Amide-I), 1530 cm^{-1} (Amide-II) and 1237 cm^{-1} (Amide-III) of band frequency were identified within the spectrum. Moreover, the 4 remaining peaks at 2929–2936 cm^{-1}, 1449 cm^{-1}, 1334 cm^{-1}, and 1091–1093 cm^{-1} frequency bands were assigned to C-H stretching, aliphatic C-H bending, CH$_2$ wagging of proline and skeletal stretching vibrations, respectively (supplementary Table 3). As illustrated in Fig. 7b–e encapsulation of gelatin beads at 5%, 10 and 15% core loading did not result in significant alteration of the FTIR spectra. Therefore, it could be suggested that encapsulation process of BGE within beads was of physical nature rather than chemical of any sort.

Thermogravimetric Analysis

Thermal behavior of bitter gourd extract, pure gelatin powder as well as empty and encapsulated gelatin beads

Fig. 6 Topographical micro images of gelatin bead without encapsulation (EGB) (**a**), with 5% core loading (GBG5%) (**b**), with 10% core loading (GBG10%) (**c**), and with 15% core loading (GBG15%) (**d**)
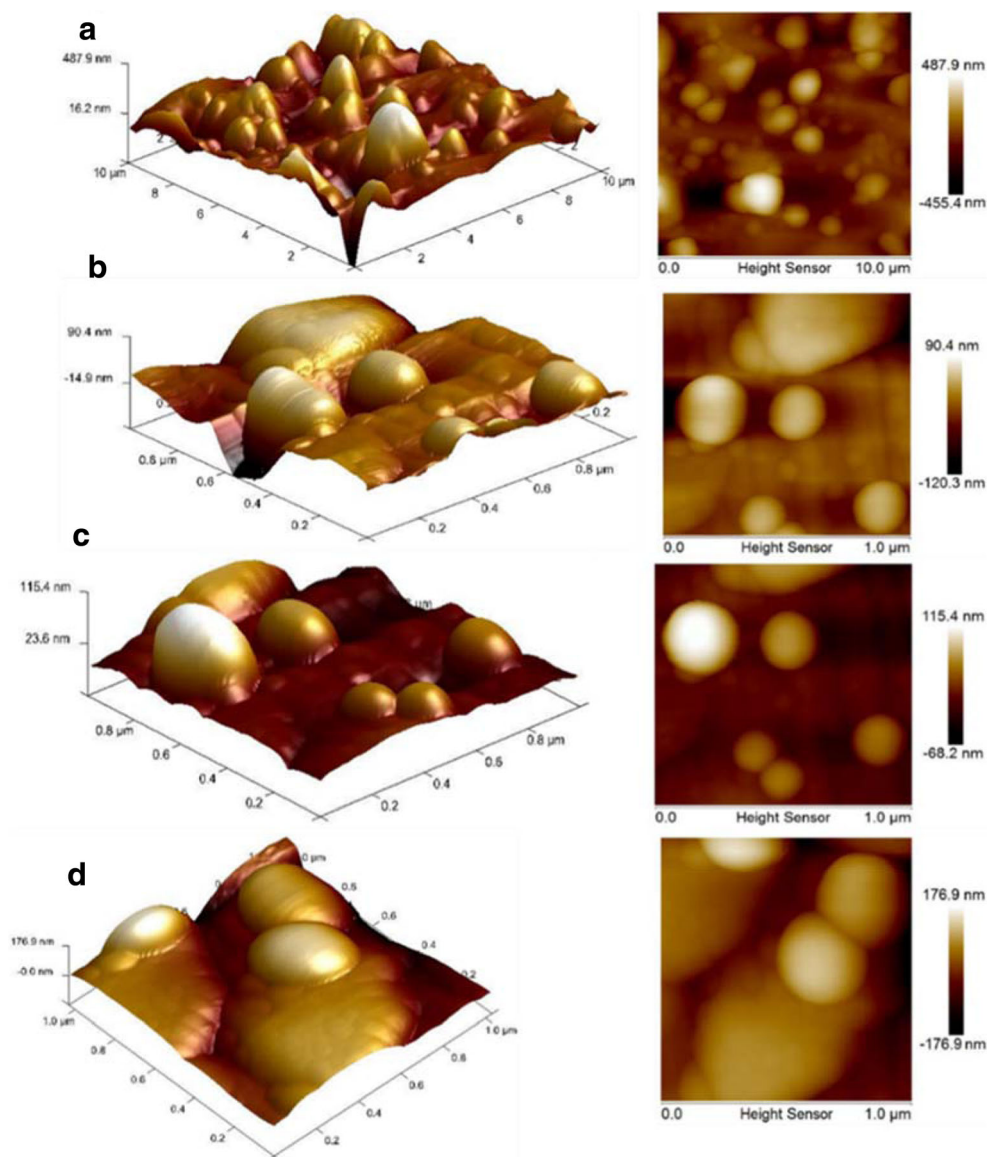
were characterized using TG-DTG thermographs. As illustrated in Fig. 8a, b, gelatin powder (GP) and EGB underwent a total of two degradation stages while GBG5%, 10 and 15% were subjected to an additional third stage. Furthermore, TGA-DTG thermographs of BGE had undergone a total of five degradation stages.

The first degradation stage for BGE (17.0%), GP (12.5%), EGB (9.0%), GBG5% (7.1%), GBG10% (8.4%), GBG 15% (7.7%) was observed over the temperature range of 28.82 °C to 144.67 °C, 29.48 °C to 227.30 °C, 29.76 °C to 163.08 °C, 28.78 °C to 140.55 °C, 29.39 °C to 138.58 °C and 29.49 °C to

Table 1 Antioxidative properties of PLE obtained bitter gourd extract (BGE extract) before and after encapsulation process

Antioxidative properties	BGE	GBG5%	GBG10%	GBG15%
TPC (g GAE/100 g sample)	5.60 ± 0.50^a	4.65 ± 0.20^b	4.75 ± 0.30^b	4.55 ± 0.40^b
TFC (g QE/100 g sample)	1.80 ± 0.10^c	1.40 ± 0.20^d	1.45 ± 0.15^d	1.32 ± 0.20^d
FRAP (µmol eq Fe (II)/gr)	780.00 ± 10.00^e	665.00 ± 20.5^f	670.00 ± 25.00^f	695.00 ± 27.00^f
IC_{50} (mg/mL)	11.50 ± 1.50^g	12.90 ± 2.00^g	13.10 ± 1.00^g	13.57 ± 1.20^g

Values are averages of triplicate analysis ± SD

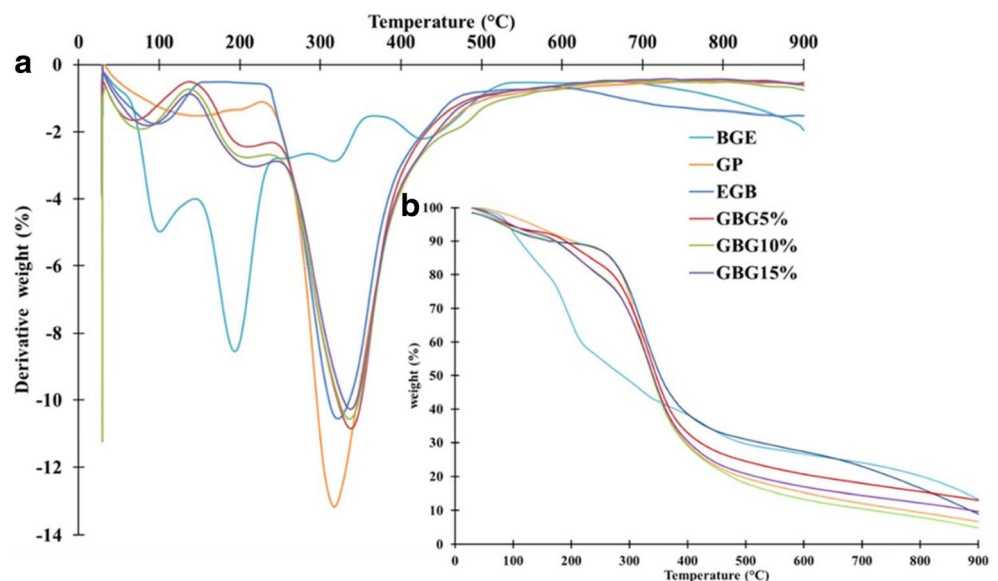Means within the rows followed by different superscript letters differ significantly at $P = 0.05$
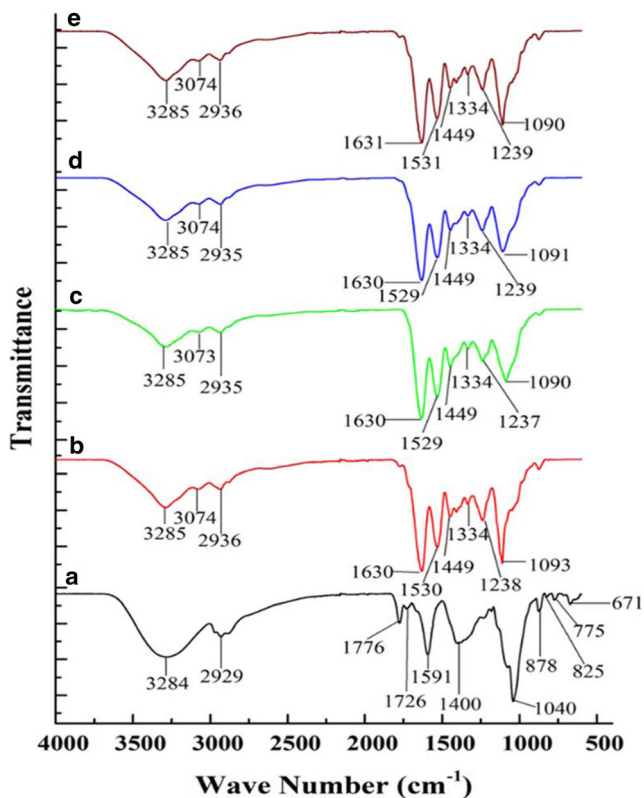
Fig. 7 FTIR spectra of bitter gourd extract (BGE) (**a**), empty gelatin bead (EGB) (**b**), gelatin beads encapsulated with 5% extract (GBG5%) (**c**), gelatin beads encapsulated with 10% extract (GBG10%) (**d**), and gelatin beads encapsulated with 15% extract (GBG15%) (**e**)

from up to 227.30 °C (in GP) to 163.08 °C (in EGB) due to electrospraying process. Furthermore, the amount of weight loss during this stage was relatively lesser in electrosprayed beads, both empty and encapsulated, in comparison to gelatin powder. This is due to fast drying of gelatin polymeric structure during electrohydrodymamic process; resulting in the removal of the structural water from the protein (Gómez-Mascaraque et al. 2015; Correia et al. 2013). Therefore, the first degradation stage observed in electrosprayed films was due to the deprivation of absorbed water. The removal of structural water from protein structure could promote hydrogen bonding occurance within the polypeptide chain (Gómez-Mascaraque et al. 2015).

Furthermore, the second degradation stage where a total of 27.33% (BGE), 82.15% (GP), and 81.24% (EGB) of polymer weight was decomposed over the temperature range of 144.67 °C to 245.85 °C, 227.30 °C to 910.14 °C and 193.08 °C to 909.77 °C, respectively. The major degradation stage of these compounds occurred within the mentioned temperature zone where the polymer backbone was thermally disassociated.

As apparent in the TGA/DTG thermographs, a decomposition stage exclusive to encapsulated beads had emerged which was not observed within EGB. This zone ranged from 140.55 °C to 241.15 °C, 138.58 °C to 238.26 °C and 138.76 °C to 248.91 °C in GBG5% (8.76%), GBG10% (10.23%) and GBG15% (12.70%), respectively. By increasing BGE content the peak area/height at approximately 200 °C, overlapped with BGE main degradation zone, increased which could be an indication of encapsulation. Neo et al. (2013) reported the appearance of gallic acid peak at 230 °C zone when

138.76 °C, respectively. The weight loss during the first stage is often associated with evaporation and deprivation of absorbed and structural water. As illustrated in Fig. 8, the first weight loss stage of gelatin polymer was reduced

Fig. 8 DTG (**a**) and TGA (**b**) thermographs of bitter gourd extract (BGE), gelatin powder (GP), empty gelatin bead (EGB), bead with 5% BGE (GBG5%), bead with 10% BGE (GBG10%), and bead with 15% BGE (GBG15%)

encapsulated within zein nanofibers through electrospinning process as well.

Moreover, final and major degradation stage of encapsulated beads occurred at an onset of 241.15 °C, 238.26 °C and 248.91 °C in GBG5%, GBG10% and GBG15%, respectively. Maximum degradation temperature (T_{max}) of encapsulated gelatin beads was within this decomposition zone, achieved at 340.80 °C (GBG5%), 338.20 °C (GBG10%) and 337.80 °C (GBG15%). These values were significantly higher ($P < 0.05$) than BGE (194.40), GP (318.50 °C) and EGB (327.12 °C) indicating encapsulation via electrospraying process increased the thermal stability of the beads.

Differential Scanning Calorimetry

The DSC heating curves of gelatin powder as well as its electrosprayed and encapsulated counterparts (5 to 15% core loading) are illustrated in Fig. 9. The glass transition temperature (T_g) and melting temperature (T_m) of GP was 89.08 °C and 191.31 °C, respectively. Electrospraying process of gelatin resulted in a decrease of T_g to 47.2 °C whereas T_m value increased to 205.9 °C. The T_g shift to a lower temperature was due to the presence of water within the nanostructure which increased polymer free volume and chain mobility (Neo et al. 2013; Hani et al. 2017). Water absorbed within the gelatin polymer structure can act as a plasticizer increasing the distance between polymer chains decreasing T_g value. Furthermore, encapsulation process of beads resulted in the disappearance of T_g which could be due to the crystalline transformation of gelatin polymer. The T_m value of beads decreased from 205.9 °C (EGB) to 155.70 °C (GBG5%), 150.28 °C (GBG10%) and 147.92 °C (GBG15%) due to encapsulation with BGE. The observed variation could be due to structural phase transition of gelatin from semi-crystalline

to crystalline phase. The crystallinity degree of GP, EBG, GBG5%, GBG10% and GBG15% was 65.20%, 42.60%, 68.60%, 69.50 and 71.50%, respectively. An increase in the crystallinity degree of gelatin bead films, due to encapsulation process, could potentially provide more suitable gas barrier properties (Biscarat et al. 2015; Ortenzi et al. 2015).
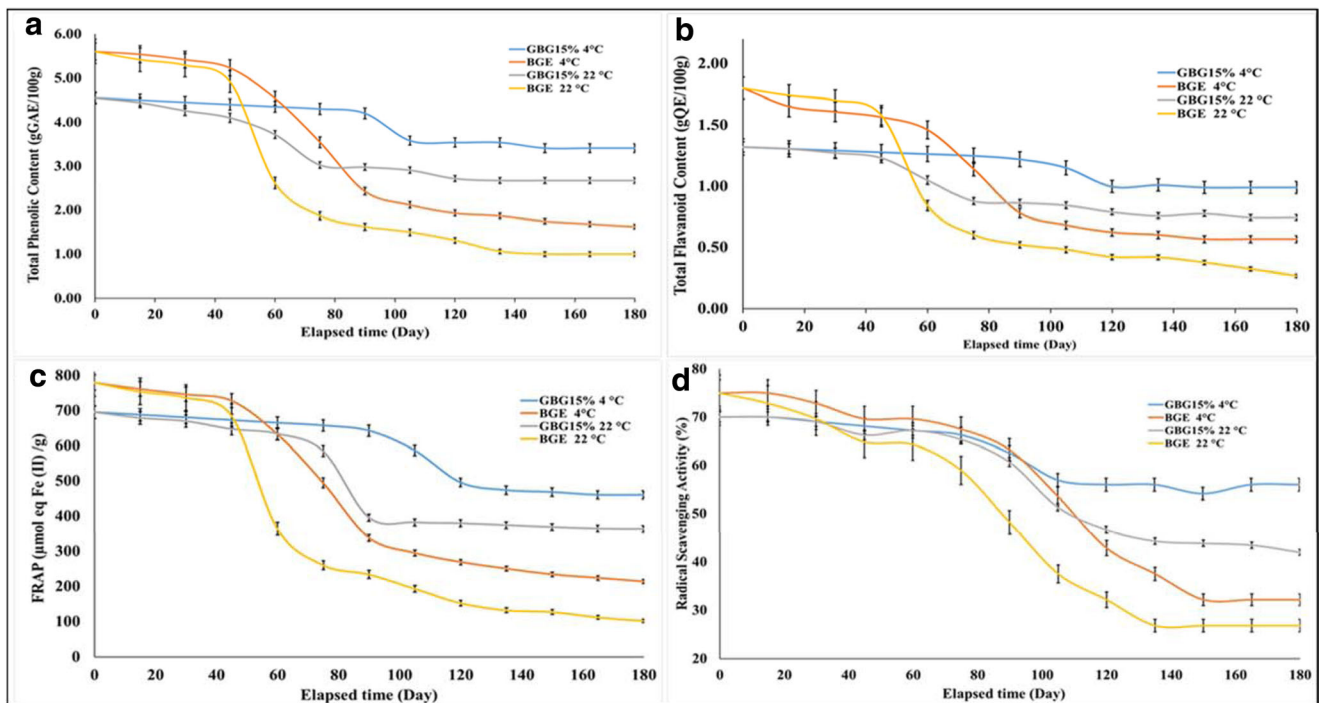
Functional Stability of Encapsulated Extracts

The effect of encapsulation and environmental parameters on phenolic content of extract and its antioxidant properties was illustrated in Fig. 10 and Online Resources 7 and 8. All three encapsulates of GBG 5%–15% followed the same trend during storage period; therefore, for simplicity GBG15% will be discussed in this section. For further information on the shelf stability of BGE and its encapsulated counterparts; please kindly refer to additional data shown in Online Resources 7 and 8.

As illustrated in Fig. 10a–d after an average of 65 days the TPC, TFC and FRAP values of BGE either stored at (BGE 22 °C) or refrigerated (BGE 4 °C) conditions decreased below their encapsulated counterparts. The RSA% value of BGE 4 °C reduced below the encapsulated values after 90 days. However, this occurrence took place after merely 50 days for its counterpart stored at ambient condition (BGE 22 °C). The TPC, FRAP and RSA% of the extract obtained from GBG15% 4 °C remained constant for a total of 90 days; whereas TFC was constant for 120 days. Given this, after 180 days of storage, the extract maintained 75%, 74%, 70 and 80% of original TPC, TFC, FRAP and RSA% of day 0, respectively. Moreover, the antioxidative content and properties of the extract obtained from the encapsulated bead film stored at ambient

Fig. 9 DSC heating curve of gelatin powder (GP), empty gelatin bead (EGB), bead with 5% BGE (GBG5%), bead with 10% BGE (GBG10%), and bead with 15% BGE (GBG15%)
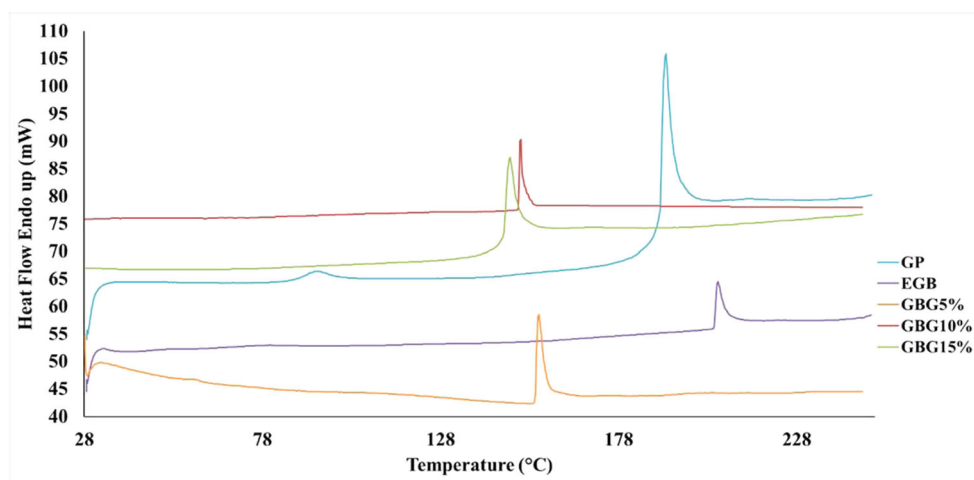
Fig. 10 Antioxidant content and functional shelf stability of PLE obtained bitter gourd extract and encapsulated beads at 15% loading

conditions (GBG15% 22 °C) started to significantly decrease after an average of 65 days. Furthermore, in all cases, the antioxidative attributes of GBG15% 4 °C and BGE 4 °C was higher than GBG 22 °C and BGE 22 °C emphasizing the importance of environmental conditions during storage.

Conclusion

The current study dealt with encapsulation of BG fruit bioactive compounds, extracted via pressurized liquid extraction, through electrospraying technique under ambient conditions. Gelatin nano beads fabricated at a concentration of 8.5% (v/w%) were found suitable to retain BGE at a core loading range of 5 to 15% (w/w). Morphological analysis illustrated that spherical geometry of beads was maintained during encapsulation process in all cases. However, increasing the core content resulted in the formation of larger bead; which was more apparently seen during the transition from 5 to 10% BGE loading. Moreover, ATR-FTIR analysis revealed that encapsulation process was more of a physical phenomenon rather than the chemical interaction between the core and wall polymer. Thermogravimetric analysis revealed encapsulation process slightly increased the thermal stability of gelatin beads to higher temperature range. Furthermore, the increased crystallinity of encapsulated gelatin bead films could potentially provide more suitable gas barrier

properties. Eventually, shelf life analysis revealed the suitability of this method to maintain antioxidant properties of BGE throughout an extended period. Therefore, it could be concluded that electrospraying technology has the potential to replace existing encapsulation methods such as spray drying for food, pharmaceutical and nutraceutical sectors.

Compliance with Ethical Standards

Conflict of Interest   The authors declare that they have no conflict of interest.

References

Anu Bhushani, J., & Anandharamakrishnan, C. (2014). Electrospinning and electrospraying techniques: Potential food based applications. *Trends in Food Science & Technology, 38*(1), 21–33.

Bakhshi, P. K., Nangrejo, M. R., Stride, E., & Edirisinghe, M. (2013). Application of electrohydrodynamic technology for folic acid encapsulation. *Food and Bioprocess Technology, 6*(7), 1837–1846.

Birnbaum, D. T., Kosmala, J. D., Henthorn, D. B., & Brannon-Peppas, L. (2000). Controlled release of β-estradiol from PLAGA microparticles: The effect of organic phase solvent on encapsulation and release. *Journal of Controlled Release, 65*(3), 375–387.

Biscarat, J., Bechelany, M., Pochat-Bohatier, C., & Miele, P. (2015). Graphene-like BN/gelatin nanobiocomposites for gas barrier applications. *Nanoscale, 7*(2), 613–618.

Budrat, P., & Shotipruk, A. (2009). Enhanced recovery of phenolic compounds from bitter melon (Momordica charantia) by subcritical water extraction. *Separation and Purification Technology, 66*(1), 125–129.

Correia, D. M., Padrão, J., Rodrigues, L. R., Dourado, F., Lanceros-Méndez, S., & Sencadas, V. (2013). Thermal and hydrolytic degradation of electrospun fish gelatin membranes. *Polymer Testing, 32*(5), 995–1000.

Dandawate, P. R., Subramaniam, D., Padhye, S. B., & Anant, S. (2016). Bitter melon: A panacea for inflammation and cancer. *Chinese Journal of Natural Medicines, 14*(2), 81–100.

Deitzel, J. M., Kleinmeyer, J., Harris, D., & Beck Tan, N. C. (2001). The effect of processing variables on the morphology of electrospun nanofibers and textiles. *Polymer, 42*(1), 261–272.

Ezhilarasi, P. N., Karthik, P., Chhanwal, N., & Anandharamakrishnan, C. (2013). Nanoencapsulation techniques for food bioactive components: A review. *Food and Bioprocess Technology, 6*(3), 628–647.

Fang, E. F., Zhang, C. Z. Y., Wong, J. H., Shen, J. Y., Li, C. H., & Ng, T. B. (2012). The MAP30 protein from bitter gourd (Momordica charantia) seeds promotes apoptosis in liver cancer cells in vitro and in vivo. *Cancer Letters, 324*(1), 66–74.

Fong, H., Chun, I., & Reneker, D. H. (1999). Beaded nanofibers formed during electrospinning. *Polymer, 40*(16), 4585–4592.

Gharsallaoui, A., Roudaut, G., Chambin, O., Voilley, A., & Saurel, R. (2007). Applications of spray-drying in microencapsulation of food ingredients: An overview. *Food Research International, 40*(9), 1107–1121.

GMIA. (1986). *Standard methods for the sampling and testing of gelatins*. New York: Gelatin Manufacturers of America Inc..

Gómez-Estaca, J., Gavara, R., & Hernández-Muñoz, P. (2015). Encapsulation of curcumin in electrosprayed gelatin microspheres enhances its bioaccessibility and widens its uses in food applications. *Innovative Food Science & Emerging Technologies, 29*, 302–307.

Gómez-Mascaraque, L. G., Lagarón, J. M., & López-Rubio, A. (2015). Electrosprayed gelatin submicroparticles as edible carriers for the encapsulation of polyphenols of interest in functional foods. *Food Hydrocolloids, 49*, 42–52.

Hani, N., Azarian, M. H., Torkamani, A. E., & Kamil Mahmood, W. A. (2016). Characterisation of gelatin nanoparticles encapsulated with Moringa oleifera bioactive extract. *International Journal of Food Science & Technology, 51*(11), 2327–2337.

Hani, N. M., Torkamani, A. E., Azarian, M. H., Mahmood, K. W. A., & Ngalim, S. H. (2017). Characterisation of electrospun gelatine nanofibres encapsulated with Moringa oleifera bioactive extract. *Journal of the Science of Food and Agriculture, 97*(10), 3348–3358.

Jaworek, A., & Sobczyk, A. T. (2008). Electrospraying route to nanotechnology: An overview. *Journal of Electrostatics, 66*(3–4), 197–219.

Kenny, O., Smyth, T. J., Hewage, C. M., & Brunton, N. P. (2013). Antioxidant properties and quantitative UPLC-MS analysis of phenolic compounds from extracts of fenugreek (Trigonella foenum-graecum) seeds and bitter melon (Momordica charantia) fruit. *Food Chemistry, 141*(4), 4295–4302.

Kriegel, C., Kit, K. M., McClements, D. J., & Weiss, J. (2009). Influence of surfactant type and concentration on electrospinning of chitosan–poly(ethylene oxide) blend nanofibers. *Food Biophysics, 4*(3), 213–228.

Lin, K.-W., Yang, S.-C., & Lin, C.-N. (2011). Antioxidant constituents from the stems and fruits of Momordica charantia. *Food Chemistry, 127*(2), 609–614.

López-Rubio, A., & Lagaron, J. M. (2011). Improved incorporation and stabilisation of β-carotene in hydrocolloids using glycerol. *Food Chemistry, 125*(3), 997–1004.

López-Rubio, A., & Lagaron, J. M. (2012). Whey protein capsules obtained through electrospraying for the encapsulation of bioactives. *Innovative Food Science & Emerging Technologies, 13*, 200–206.

López-Rubio, A., Sanchez, E., Wilkanowicz, S., Sanz, Y., & Lagaron, J. M. (2012). Electrospinning as a useful technique for the encapsulation of living bifidobacteria in food hydrocolloids. *Food Hydrocolloids, 28*(1), 159–167.

Mit-uppatham, C., Nithitanakul, M., & Supaphol, P. (2004). Ultrafine electrospun polyamide-6 fibers: Effect of solution conditions on morphology and average fiber diameter. *Macromolecular Chemistry and Physics, 205*(17), 2327–2338.

Neo, Y. P., Ray, S., Jin, J., Gizdavic-Nikolaidis, M., Nieuwoudt, M. K., Liu, D., & Quek, S. Y. (2013). Encapsulation of food grade antioxidant in natural biopolymer by electrospinning technique: A physicochemical study based on zein–gallic acid system. *Food Chemistry, 136*(2), 1013–1021.

Norziah, M. H., Al-Hassan, A., Khairulnizam, A. B., Mordi, M. N., & Norita, M. (2009). Characterization of fish gelatin from surimi processing wastes: Thermal analysis and effect of transglutaminase on gel properties. *Food Hydrocolloids, 23*(6), 1610–1616.

Ortenzi, M. A., Basilissi, L., Farina, H., Di Silvestro, G., Piergiovanni, L., & Mascheroni, E. (2015). Evaluation of crystallinity and gas barrier properties of films obtained from PLA nanocomposites synthesized via "in situ" polymerization of l-lactide with silane-modified nanosilica and montmorillonite. *European Polymer Journal, 66*, 478–491.

Pérez-Masiá, R., Lagaron, J. M., & López-Rubio, A. (2014). Development and optimization of novel encapsulation structures of interest in functional foods through electrospraying. [journal article]. *Food and Bioprocess Technology, 7*(11), 3236–3245.

Pérez-Masiá, R., López-Nicolás, R., Periago, M. J., Ros, G., Lagaron, J. M., & López-Rubio, A. (2015). Encapsulation of folic acid in food hydrocolloids through nanospray drying and electrospraying for nutraceutical applications. *Food Chemistry, 168*, 124–133.

Syahariza, Z. A., Torkamani, A. E., Norziah, H. M., Mahmood, W. A. K., & Juliano, P. (2017). Optimisation of pressurised liquid extraction for antioxidative polyphenolic compound from Momordica charantia using response surface methodology. *International Journal of Food Science & Technology, 52*(2), 480–493.

Xu, Y., & Hanna, M. A. (2006). Electrospray encapsulation of water-soluble protein with polylactide: Effects of formulations on morphology, encapsulation efficiency and release profile of particles. *International Journal of Pharmaceutics, 320*(1), 30–36.

Zhou, P., & Regenstein, J. M. (2005). Effects of alkaline and acid pretreatments on Alaska Pollock skin gelatin extraction. *Journal of Food Science, 70*(6), 392–396.